Energy scales in the Raman spectrum of electron- and hole-doped cuprates within competing scenarios

B. Valenzuela[1,2,*] and E. Bascones[1]

[1]*Instituto de Ciencia de Materiales de Madrid, CSIC, Cantoblanco, E-28049 Madrid, Spain*

[2]*Departamento de Física de la Materia Condensada, Universidad Autónoma de Madrid, Cantoblanco, E-28049 Madrid, Spain*

(Received 16 June 2008; revised manuscript received 3 October 2008; published 21 November 2008)

Recent experiments in underdoped hole-doped cuprates have shown the presence of two energy scales in the Raman spectrum in the superconducting state. This feature has a natural explanation in some models in which pseudogap and superconductivity compete. In electron-doped cuprates antiferromagnetic correlations are believed to survive in the superconducting state and are believed to produce a pseudogap above the critical temperature. Contrary to hole-doped systems, in electron-doped compounds only one energy scale appears since the pair-breaking Raman intensity peaks in both B_{1g} (antinodal) and B_{2g} (nodal) channels at a frequency of a few meV, typical of the superconducting order parameter. In this paper we analyze the different effects in the Raman spectrum of the competition between pseudogap and superconductivity in electron- and hole-doped cuprates. The difference in energy scales in both systems is explained in terms of the different truncation of the Fermi surface induced by the pseudogap. For electron-doped cuprates we also analyze the spectrum with antiferromagnetism and a nonmonotonic superconducting order parameter.

DOI: 10.1103/PhysRevB.78.174522 PACS number(s): 74.72.−h, 71.10.−w, 78.20.Bh

I. INTRODUCTION

The pseudogap (PG) and the asymmetry between electron- and hole-doped cuprates are key issues in high-temperature superconductivity. In angle-resolved photoemission spectroscopy (ARPES) in hole-doped compounds, the PG manifests in reduced intensity in the antinodal region [close to $(0,\pi)$] and a Fermi arc in the nodal one [around $(\pi/2,\pi/2)$] instead of a complete Fermi surface[1] (FS). Recent ARPES (Ref. 2) and Raman[3] experiments suggest that the nodal-antinodal dichotomy remains in the superconducting (SC) state in the form of two energy scales.

Inelastic Raman scattering[4] permits differentiating of the zero-momentum charge excitations of nodal ($\chi_{B_{2g}}$) and antinodal regions ($\chi_{B_{1g}}$). In the SC state, pair-breaking peaks appear in the Raman spectrum. In hole-doped cuprates the B_{2g} peak frequency shows a nonmonotonic dependence on doping x, similar to that of the critical temperature T_c. On the contrary, the B_{1g} intensity strongly decreases with underdoping with a peak frequency which seems to evolve from the SC to the PG scale.[3,5] This behavior has been interpreted as a signature of the competition between SC and PG.[5,6] For alternative descriptions, see Refs. 3 and 7. Very recent measurements[8] show that in underdoped compounds the position of the B_{1g} peak barely changes with temperature and that intensity at this frequency remains above T_c, opposite to what happens in overdoped samples. It also appears at the same frequency in impurity-substituted samples with different T_c but the same nominal doping.[9] On the contrary, the nodal B_{2g} peak displays a significant temperature dependence below T_c in both the underdoped and the overdoped regimes.[10]

In electron-doped cuprates the PG suppresses the ARPES intensity at the hot spots,[11] where the FS cuts the antiferromagnetic zone border (AFZB). This suppression remains in the SC state. Band folding across the AFZB (Refs. 12) and a gap of ~100 meV at the hot spots have been observed.[12–14] This gap remains in the superconducting state. These features are well reproduced by a spin-density wave (SDW) state and its coexistence with superconductivity below T_c.[15,16] The SDW model[17] is based on an itinerant electron approach to the antiferromagnetism. The SDW truncates the FS into electron and hole pockets at the antinodal and nodal regions. The pockets picture and the AF origin[18] of the PG agrees with the doping evolution of the Hall coefficient,[19] the elastic peaks at $\mathbf{Q}=(\pi,\pi)$ observed in neutron scattering,[20] magnetotransport,[21] and optical conductivity[22] experiments.

Contrary to hole-doped materials, in electron-doped compounds the pair-breaking Raman intensity peaks in both B_{1g} (antinodal) and B_{2g} (nodal) channels at a frequency of a few meV, typical of the SC order parameter.[23,24] The peak frequency has a nonmonotonic dependence on doping, similar to that of T_c. For some dopings, B_{2g} peaks at a frequency larger than B_{1g}, which has been interpreted in terms of a nonmonotonic d-wave SC gap[23,25,26] with maximum value at the hot spots.[27] A nonmonotonic leading edge shift below T_c was observed[28,29] in samples which show a gap of 100 meV at the hot spots above and below the critical temperature. Yuan *et al.*[30] and Liu *et al.*,[31] respectively, proposed that the nonmonotonicity of the ARPES gap and the relative position of the B_{1g} and B_{2g} peaks were a consequence of the coexistence of antiferromagnetism and d-wave superconductivity. In electron-doped cuprates the SDW and SC scales can be decoupled.[32] The different values of SC scale[28,33] (~4 meV) with respect to the pseudogap (~100 meV) suggest that the nonmonotonicity is not associated with the opening of an antiferromagnetic gap.[34] In the presence of a PG as the one seen in ARPES,[12,13] the Raman spectrum including both SDW and a nonmonotonic d-wave gap should be studied.

In this paper we analyze the different Raman spectrum of electron- and hole-doped cuprates within competing scenarios. In electron-doped cuprates the PG is modeled by a SDW and it is assumed to remain present in the SC

state.[15,16,30] For hole-doped systems we use the Yang-Rice-Zhang (YRZ) model[35] which reproduces well[5] the doping dependencies of B_{1g} and B_{2g} peak frequencies and intensities. As it is also experimentally observed, in the hole-doped superconductors the PG scale couples with the SC one and affects the pair-breaking Raman spectrum while PG and SC scales are decoupled in electron-doped compounds. We show that such a difference is not a consequence of the different model used but of the different region of the Fermi surface which is truncated by the pseudogap. We also calculate the Raman spectrum corresponding to a nonmonotonic SC d-wave gap in the presence of a SDW to make a closer comparison with experiments.

II. MODEL

A. Electron-doped cuprates

We start from the Green's function in the presence of antiferromagnetism and superconductivity which couples the operators $(c^{\dagger}_{\mathbf{k},\uparrow}, c_{-\mathbf{k},\downarrow}, c^{\dagger}_{\mathbf{k}+\mathbf{Q},\uparrow}, c_{-\mathbf{k}-\mathbf{Q},\downarrow})$

$$\mathbf{G}^{-1}(\omega,\mathbf{k}) = \begin{pmatrix} \omega-\xi_{\mathbf{k}} & -\Delta_{S,\mathbf{k}} & -\Delta_{\mathrm{AF}} & 0 \\ -\Delta_{S,\mathbf{k}} & \omega+\xi_{\mathbf{k}} & 0 & -\Delta_{\mathrm{AF}} \\ -\Delta_{\mathrm{AF}} & 0 & \omega-\xi_{\mathbf{k}+\mathbf{Q}} & -\Delta_{S,\mathbf{k}+\mathbf{Q}} \\ 0 & -\Delta_{\mathrm{AF}} & -\Delta_{S,\mathbf{k}+\mathbf{Q}} & \omega+\xi_{\mathbf{k}+\mathbf{Q}} \end{pmatrix}.$$

Such a Green's function can be derived from the Hubbard or $t-J$ model at mean-field level.[15,16,30] We assume a doping dependent[16] isotropic AF gap Δ_{AF} and a d-wave SC order parameter $\Delta_{S,\mathbf{k}}=(\Delta_S/2)(\cos k_x-\cos k_y)$ except otherwise indicated. The band dispersion is $\xi_{\mathbf{k}}=-2t_0(\cos k_x+\cos k_y) -4t_1 \cos k_x \cos k_y-2t_2(\cos 2k_x+\cos 2k_y)-\mu$.

Next we consider the Raman response. We use the symmetry of the point-group transformations of the crystal to classify the scattering amplitude.[36] Since we are mostly concerned in the anisotropic properties of the system, we will calculate the B_{1g} and the B_{2g} channels and not the A_{1g} channel. This will be also valid for the hole-doped case. In the bubble approximation the Raman response is

$$\chi^{\nu}(\Omega) = \frac{1}{N}\sum_{\mathbf{k}} (\gamma^{\nu}_{\mathbf{k}})^2\{\Pi_{11,11}(\mathbf{k},\Omega) - \Pi_{12,21}(\mathbf{k},\Omega) + (-1)^{\eta}[\Pi_{13,31}(\mathbf{k},\Omega) - \Pi_{14,41}(\mathbf{k},\Omega)]\}, \quad (1)$$

$$\Pi_{ij,kl}(\mathbf{k},i\Omega) = T\sum_{n} G_{ij}(i\omega_n + i\Omega,\mathbf{k})G_{kl}(i\omega_n,\mathbf{k}). \quad (2)$$

Here $\gamma_{B_{1g}} \propto (\cos k_x - \cos k_y)$ and $\gamma_{B_{2g}} \propto (\sin k_x \sin k_y)$ are the Raman vertices,[37] $\eta=1,2$, respectively, for B_{1g} and B_{2g}, and the Green's functions are written in the extended Brillouin zone. Equivalent expressions apply[6] for coexisting d-density wave and SC. At zero temperature and zero scattering rate,

$$\chi^{B_{2g}}(\Omega) = \frac{1}{4}\sum_{\mathbf{k},\tau=\pm} (\gamma^{B_{2g}}_{\mathbf{k}})^2 \frac{\Delta^2_{S,\mathbf{k}}}{(E^{\tau}_{\mathbf{k}})^2}\left(1+\frac{\tau\xi^{-}_{\mathbf{k}}}{E_{\mathbf{k}}}\right)\delta(\Omega-2E^{\tau}_{\mathbf{k}}), \quad (3)$$

$$\chi^{B_{1g}}(\Omega) = \frac{1}{4}\sum_{\mathbf{k}} (\gamma^{B_{1g}}_{\mathbf{k}})^2 \left\{ \frac{\Delta^2_{\mathrm{AF}}}{E^2_{\mathbf{k}}}\Lambda_{\mathbf{k}}\delta(\Omega-E^{+}_{\mathbf{k}}-E^{-}_{\mathbf{k}}) + \sum_{\tau=\pm} \frac{\Delta^2_{S,\mathbf{k}}}{(E^{\tau}_{\mathbf{k}})^2}\left(1+\frac{\tau\xi^{-}_{\mathbf{k}}}{E_{\mathbf{k}}}\right)\left(\frac{\tau\xi^{-}_{\mathbf{k}}}{E_{\mathbf{k}}}\right)\delta(\Omega-2E^{\tau}_{\mathbf{k}}) \right\}, \quad (4)$$

with $\Lambda_{\mathbf{k}}=(1-\frac{(\xi^{+}_{\mathbf{k}})^2+\Delta^2_{S,\mathbf{k}}-E^2_{\mathbf{k}}}{E^{+}_{\mathbf{k}}E^{-}_{\mathbf{k}}})$, $\xi^{\pm}_{\mathbf{k}}=(1/2)(\xi_{\mathbf{k}}\pm\xi_{\mathbf{k}+\mathbf{Q}})$, $E^{\pm}_{\mathbf{k}} =[(\xi^{+}_{\mathbf{k}}\pm E_{\mathbf{k}})^2+(\Delta_{S,\mathbf{k}})^2]^{1/2}$, and $E_{\mathbf{k}}=[(\xi^{-}_{\mathbf{k}})^2+\Delta^2_{\mathrm{AF}}]^{1/2}$. In the calculations we use Eq. (1) with a constant scattering rate Γ except otherwise stated. A more proper treatment of the scattering rate should include the effects of impurities, inelastic scattering, disorder, and the well-known flat background at high frequencies but it is beyond the scope of this article.[38]

B. Hole-doped cuprates

We use the Yang-Rice-Zhang model[35] to describe the pseudogap in hole-doped cuprates. This model assumes that the pseudogap state can be described as doped resonant valence bond (RVB) state and proposes an ansatz for the coherent part of the single-particle Green's function to characterize it. This ansatz was proposed in analogy with the form derived for a doped spin liquid formed by an array of two-leg Hubbard ladders near half filling. The description starts from $t-J$ model and uses the Gutzwiller approximation to project out double occupied sites as in the early renormalized mean-field description of the RVB state.[39] In particular the kinetic energy (i.e., the values of the hopping parameters) and the coherent quasiparticle spectral weight are renormalized via $g_t=2x/(1+x)$, and depend on doping. We use the doping dependence of the hopping parameters proposed in Ref. 35. A feature of the YRZ model is to describe the pseudogap correlations at zero temperature by a parameter Δ_R via a self energy $\Sigma_R(\mathbf{k},\omega)=\Delta^2_{R,\mathbf{k}}/(\omega+\xi_{0\mathbf{k}})$ which diverges at zero frequency at the umklapp surface $\xi_{0\mathbf{k}}$ (Luttinger surface). Here $\xi_{0\mathbf{k}}=-2t_0(x)(\cos k_x+\cos k_y)$ and $\Delta_{R,\mathbf{k}}=[\Delta_R(x)/2](\cos k_x-\cos k_y)$. Hole pockets appear close to $(\pm\pi/2,\pm\pi/2)$ but Δ_R does not break any symmetry. In the superconducting state of underdoped cuprates, coexistence of pseudogap and superconductivity is assumed. The diagonal element of the matrix Green's function becomes

$$G^{\mathrm{RVB}}_{\mathrm{SC}}(\mathbf{k},\omega) = \frac{g_t}{\omega-\xi(\mathbf{k})-\Sigma_R(\mathbf{k},\omega)-\Sigma_S(\mathbf{k},\omega)}. \quad (5)$$

with $\xi_{\mathbf{k}}=\xi_{0\mathbf{k}}-4t_1(x)\cos k_x \cos k_y-2t_2(x)(\cos 2k_x+\cos 2k_y) -\mu_p$ and μ_p determined from the Luttinger sum rule. $\Sigma_S(\mathbf{k},\omega)=|\Delta^2_{S,\mathbf{k}}|/[\omega+\xi(\mathbf{k})+\Sigma_R(\mathbf{k},-\omega)]$ is the superconducting self energy with $\Delta_{S,\mathbf{k}}=[\Delta_S(x)/2](\cos k_x-\cos k_y)$ as the superconducting order parameter. In the pseudogap state there are two quasiparticle bands with strongly varying spectral weight. These two bands become four in the superconducting state, $\pm E^{\pm,h}_{\mathbf{k}}$ (Refs. 5 and 35):

$$(E^{\pm,h}_{\mathbf{k}})^2 = \Delta^2_{R,\mathbf{k}} + \frac{\xi^2_{\mathbf{k}}+\xi^2_{0\mathbf{k}}+\Delta^2_{S,\mathbf{k}}}{2} \pm (E^{\mathrm{SC},h}_{\mathbf{k}})^2,$$

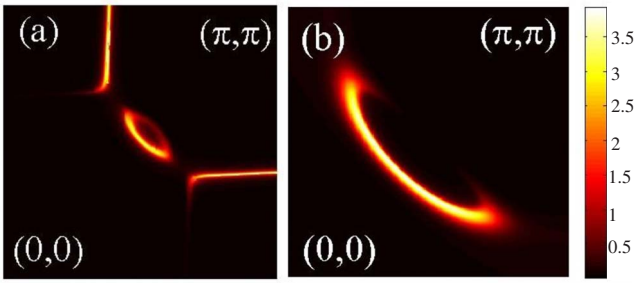

FIG. 1. (Color online) Simulated map of ARPES intensity at the Fermi energy with $\Gamma=0.02$ for electron-doped cuprates in (a) and hole-doped cuprates in (b) for the parameters given in the text. The spectral function is convoluted with a Gaussian of width of 0.06 to mimic finite resolution.

$$(E_{\mathbf{k}}^{\mathrm{SC},h})^2 = \sqrt{(\xi_{\mathbf{k}}^2 - \xi_{0\mathbf{k}}^2 + \Delta_{S,\mathbf{k}}^2)^2 + 4\Delta_{R,\mathbf{k}}^2[(\xi_{\mathbf{k}} - \xi_{0\mathbf{k}})^2 + \Delta_{S,\mathbf{k}}^2]}.$$

The Raman spectrum is calculated in the bubble approximation as in Ref. 5.

C. Parameters

In both electron- and hole-doped cuprates, the PG scales Δ_{AF} and Δ_R decrease with doping and vanish at a quantum critical point (QCP), at which Fermi liquid and BCS description are recovered in the normal and superconducting states, respectively. In hole-doped compounds the hopping parameters are renormalized according to the Gutzwiller approximation and depend also on doping.[35] In order to compare the behavior in electron- and hole-doped systems, we keep the doping constant and equal to $x=0.13$ for electron-doped case and $x=0.14$ in the hole-doped case, and vary Δ_S. We work in units of the unrenormalized nearest-neighbor hopping $t=1$. For electron-doped cuprates we use $t_0=1$, $t_1=-0.3$, $t_2=0.25$, $\Delta_{\mathrm{AF}}=0.3$, and $\mu=0.59$, corresponding to $x=0.13$, which reproduces well the ARPES intensity at the Fermi level [Fig. 1(a)]. In hole-doped cuprates we use $t_0=0.37$, $t_1=-0.073$, $t_2=0.05$, $\Delta_R=0.18$, and $\mu_p=-0.29$. The ARPES intensity corresponding to these values is shown in Fig. 1(b). The parameters chosen reproduce reasonably well the ARPES spectrum for both electron- and hole-doped cuprates. However they are not expected to give a quantitative fitting of the Raman spectrum. In the hole-doped case the parameters chosen are the ones originally proposed in the paper by Yang *et al.*,[35] and later used in Refs. 5 and 40. To better compare with the hole-doped case and for numerical convenience, the superconducting order parameter in the electron-doped case is larger than the experimental one. Our emphasis is in the qualitatively different behavior observed in the Raman spectrum of electron- and hole-doped cuprates.

The aim of this paper is to compare the qualitative changes of the Raman spectrum when going from the normal pseudogap to the superconducting state. Experimentally the normal state is reached with increasing temperature above T_c. On the other hand, the YRZ model used for hole-doped cuprates, based on the Gutzwiller projection, was developed only for zero temperature. To mimic the effect of going from the superconducting to the normal state, we vary Δ_S, keeping the temperature equal to zero and the PG scale, Δ_{AF}, or Δ_R constant. We believe that the qualitative features described in this paper will be present when going from the superconducting to the normal state by increasing the temperature.

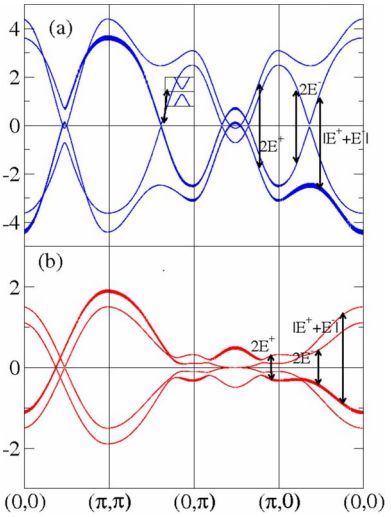

FIG. 2. (Color online) Energy bands in the superconducting state corresponding to the parameters given in the text for (a) electron-doped and (b) hole-doped cuprates. The inset in (a) zooms the opening of the superconducting gap at the electron pocket along $(0,\pi)-(\pi,\pi)$. The width of the bands gives an idea of the corresponding spectral weight. The arrows show the possible interband transitions.

III. RAMAN SPECTRUM

A. Electron-doped cuprates

With SC and SDW the energy spectrum consists of four bands with energies $\pm|E_{\mathbf{k}}^{\pm}|$ [see Fig. 2(a)]. The pair-breaking excitations due to superconductivity are given by the terms with $\delta(\Omega-2E_{\mathbf{k}}^{\pm})$ in Eqs. (3) and (4). These terms describe two different transitions, shown on the right side of Fig. 2(a), with energies $\Omega=2E_{\mathbf{k}}^{\pm}$. Sketched in the figure, there is a third kind of interband transition with $\Omega=E_{\mathbf{k}}^{+}+E_{\mathbf{k}}^{-}$. Its contribution to the Raman spectrum is given by the first term in Eq. (4). In contrast to pair-breaking excitations, it is not SC induced but it has an SDW origin. A similar transition shows up also in the Raman response of a SDW in the absence of SC ($\Delta_S=0$). Thus this transition remains above T_c if the temperature at which the AF order appears is larger than T_c. As pointed out in Ref. 32, the SDW-induced peak is only seen in B_{1g} and not in B_{2g}, both with and without superconductivity. The corresponding term is missing in Eq. (3). This is a consequence of the breaking of symmetry produced by the SDW, and how this symmetry breaking relates to the polarization of B_{1g} and B_{2g} channels. The different behavior in both channels arises from the sign which precedes the $\Pi_{13,31}-\Pi_{14,41}$ term in Eq. (1). Its contribution to the SDW-induced transition is equal, in absolute value, to that of $\Pi_{11,11}-\Pi_{12,21}$. For B_{1g} polarization both contributions add while for B_{2g} they cancel each other. This result also applies to other charge or spin-density wave phases with $\mathbf{Q}=(\pi,\pi)$.[6]

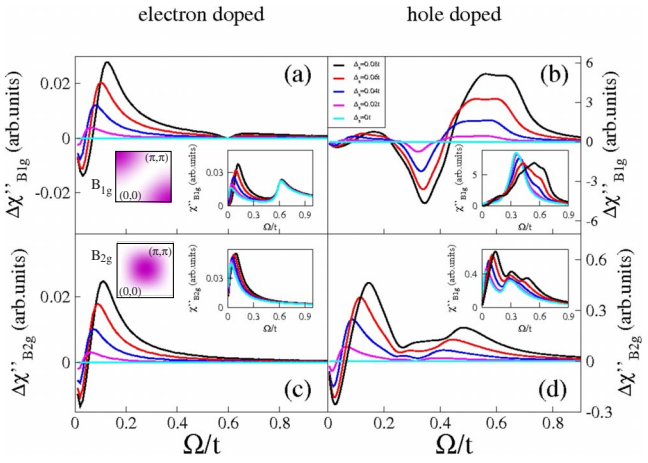

FIG. 3. (Color online) Raman response in B_{1g} (top) and B_{2g} (bottom) channels in electron-doped (left) and hole-doped (right) cuprates as a function of the superconducting order parameter Δ_S. The insets show the total response $\chi''_{B_{1g},B_{2g}}$ and the main figures show the difference one $\Delta\chi''_{B_{1g},B_{2g}}=\chi''_{B_{1g},B_{2g}}(\Delta_S)-\chi''_{B_{1g},B_{2g}}(\Delta_S=0)$. Intensity is in arbitrary units. Γ is given in units of the unrenormalized nearest-neighbor hopping parameter

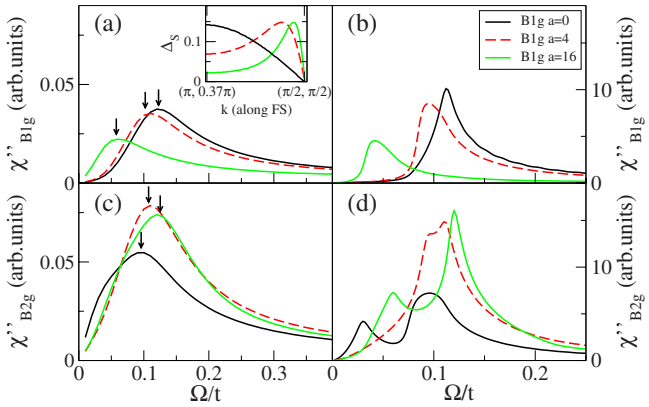

FIG. 4. (Color online) [(a) and (c)] B_{1g} and B_{2g} Raman responses calculated with Γ=0.02 and corresponding to different anisotropies of the order parameter given in Eq. (6) with **k** dependence along the Fermi surface (in the absence of SDW gap) is given in the inset. [(b) and (d)] Pair breaking peaks corresponding to the same values as in left figures. This figure has been calculated using Eqs. (3) and (4) and introducing a broadening of 0.001 to the δ function. In all the figures $a=0$ (black solid), $a=4$ (red dashed), and $a=16$ (light green solid). Γ and the broadening of the δ function are measured in units of the unrenormalized nearest-neighbor hopping parameter. The spectrum is given in arbitrary units.

The total Raman spectrum is plotted in the left insets of Figs. 3(a) and 3(c) for different values of Δ_S. A peak at about $2\Delta_S$ due to pair-breaking excitations is observed in both B_{1g} and B_{2g} channels. Its intensity decreases and its position shifts to lower energies as Δ_S decreases, in a way which resembles what happens in a BCS superconductor with $\Delta_{AF}=0$. The low-energy feature in the $\Delta_S=0$ curve in both electron- and hole-doped cuprates corresponds to the Drude peak. Compared to the BCS spectrum, at low energies the presence of the SDW suppresses slightly the intensity in the B_{1g} channel since some of the spectral weight is reorganized due to the opening of the SDW. The missing spectral weight is found in the SDW-induced peak at higher energies. In B_{2g} the linear Ω dependence at low energies, characteristic of a SC gap with nodes, is observed. Closer inspection (see black curves in the right panels of Fig. 4) shows that the pair-breaking feature in B_{2g} has a double-peak structure. The double-peak structure originates in the two transitions with energies $|2E^+_{\mathbf{k}}|$ and $|2E^-_{\mathbf{k}}|$ discussed above. The double peaks appear in both B_{1g} and B_{2g} Raman responses although in B_{1g}, one of the peaks is very much suppressed and cannot be resolved at the scales shown in the figures. Both peaks are very close in frequency and the scattering rate makes them merge into a single one, as can be appreciated in the B_{2g} response (black dashed curve) of Fig. 4(a). The peak at $\Omega=2\Delta_{AF}$ in the B_{1g} spectrum arises from the SDW-induced transition.

The effect of superconductivity in the Raman spectrum is better seen in the main figures in Figs. 3(a) and 3(c), where the response in the SDW-normal state has been subtracted. Except for the suppression of intensity in the B_{1g} spectrum at $\Omega=2\Delta_{AF}$, no feature shows up in the subtracted figures at the SDW energy scale. This dip in intensity is due to the $\left(\frac{\tau\tilde{\xi}_{\mathbf{k}}}{E_{\mathbf{k}}}\right)$ factor in Eq. (4) which makes the contribution of the hot spots to the pair-breaking B_{1g} intensity vanish. In the difference spectra the peaks in B_{1g} and B_{2g} appear at the same energy scale and have a similar dependence on Δ_S. Below we show that this is not the case in hole-doped cuprates.

B. Hole-doped cuprates

As to the case of electron-doped cuprates discussed above, the energy spectrum is composed of four bands with energies $\pm E^{\pm,h}_{\mathbf{k}}$ [see Fig. 2(b)], whose expressions are given by Eq. (6). The Raman spectrum is composed of three transitions: two pair-breaking peaks with energies $2|E^{-,h}_{\mathbf{k}}|$ and $2|E^{+,h}_{\mathbf{k}}|$, and a third *crossing* transition with energy $|E^{-,h}_{\mathbf{k}}+E^{+,h}_{\mathbf{k}}|$. The *crossing* transition is associated to the PG correlations in a similar way as the SDW transition in the electron-doped materials is associated to antiferromagnetism. However, in the hole-doped case, Δ_R does not break any symmetry, Π_{13} and Π_{14} vanish, and the *crossing* transition is active in both B_{1g} and B_{2g}.

The Raman spectrum shown in the right insets of Figs. 3(b) and 3(d) differs considerably with respect to that of electron-doped cuprates. Two peaks appear in B_{2g} channel. The low-frequency one shifts to lower frequencies and decreases in intensity with decreasing Δ_S, as expected for a pair-breaking peak. The intensity of the weaker high-frequency peak also decreases with decreasing Δ_S. At $\Delta_S=0$ its intensity is finite and comes from the *crossing* transition discussed above. Note that as in the electron-doped case the low-energy peak which appears for $\Delta_S=0$ is due to a finite value of Γ.

The increase in the high-frequency peak intensity with increasing Δ_S indicates that pair-breaking excitations also contribute to the intensity at this frequency in the superconducting state. The B_{1g} response is dominated by the high-frequency peak whose intensity is reorganized in the superconducting state. The low-frequency feature appears just as a

small shoulder in the total spectrum. Interestingly, as experimentally observed[8] all the curves seem to cross at a single point (isosbestic point).

Main figures in Figs. 3(b) and 3(d) show the difference response $\Delta\chi''_{B_{1g},B_{2g}}=\chi''_{B_{1g},B_{2g}}(\Delta_S)-\chi_{B_{1g},B_{2g}}$ $(\Delta_S=0)$. The B_{2g} spectrum is dominated by the low-frequency peak. However a smaller peak at high frequency can be also discerned. The low- and high-frequency peaks in the difference curves are both pair breaking and correspond, respectively, to the $|2E^-_{\mathbf{k}}|$ and $|2E^+_{\mathbf{k}}|$ transitions. The characteristic energy scales of the peaks differ strongly from the ones found in the electron-doped case in which both pair-breaking peaks appeared at a scale given by Δ_S and could barely be distinguished. The features in the B_{1g} difference spectrum differ from those found in B_{2g}. The low-frequency feature is very weak while the high-frequency pair-breaking peak dominates the response. The last one is wide and its position does not change much with Δ_S. Note that, because the position in frequency at which the *crossing* and high-frequency pair-breaking transitions peak are so close, intensity at this energy is also expected in the PG state in the absence of superconductivity.

IV. NONMONOTONIC SUPERCONDUCTING GAP IN ELECTRON-DOPED CUPRATES

As discussed in the previous section, at the bubble level even in the presence of a SDW using a *d*-wave form for the superconducting order parameter, the B_{2g} pair-breaking contribution peaks at a frequency smaller than the B_{1g} one, contrary to what was observed at optimal doping in electron-doped cuprates.[23,24] A nonmonotonic *d*-wave SC gap is a plausible explanation for the observed peak position. The spectrum for a nonmonotonic SC *d*-wave gap, in the absence of antiferromagnetism, was reported in Ref. 25. In Fig. 4 we plot the spectrum for coexisting SDW and a nonmonotonic SC order parameter.[25] Here,

$$\Delta_{S,\mathbf{k}}=\Delta_0\frac{\sqrt{a}}{3\sqrt{3}}\frac{\cos k_x-\cos k_y}{[1+a/4(\cos k_x-\cos k_y)^2]^{3/2}}, \qquad (6)$$

for $a=4,16$ whose $\mathbf{k}$ dependence is given in the inset and is compared with the spectrum for pure *d*-wave Δ_S. All the Raman spectra shown in this figure correspond to the same maximum value $\Delta_{\max}$ but its position shifts toward the node with increasing *a*. Left panels show the spectrum calculated with $\Gamma=0.02$, the value for which the two pair-breaking peaks cannot be resolved (as expected experimentally). With increasing *a* the position of the B_{2g} peak shifts to larger frequency while the peak intensity increases. On the other hand the position of the B_{1g} peak shifts to lower frequency and the peak intensity decreases. This behavior is expected from the generic form of the gap and differs little from the one found for a nonmonotonic *d*-wave gap in the absence of a SDW.[25] These features are in agreement with the experimental results. The effect of the SDW is better seen in the right panels which have been calculated using Eqs. (3) and (4) adding a small broadening to the δ function. With increasing *a* the lowest (highest) pair-breaking peak shifts to higher (lower) frequency. As a consequence, with increasing nonmonotonicity (increasing *a*) the peaks first merge together $(a=4)$ and then exchange positions $(a=16)$. Due to the similarity of the spectrum with and without SDW, it is not possible to extract any fingerprint of the SDW from the low-energy Raman spectrum.

V. SUMMARY AND DISCUSSION

We have analyzed how pseudogap and superconducting scales show up in the Raman spectrum of electron- and hole-doped cuprates. The pseudogap in electron-doped compounds was described by a spin-density wave model while for hole-doped cuprates, we have used the Yang-Rice-Zhang model for a doped spin liquid. In both cases the pseudogap was assumed to remain in the superconducting state and compete with superconductivity, removing part of the underlying Fermi surface. Below T_c, superconductivity induces pair-breaking peaks in the Raman spectrum. Due to the modification of the energy spectrum, in the presence of the PG the typical BCS pair-breaking peak splits into two.

The two pair-breaking peaks are very close in frequency in electron-doped systems. One of the peaks is strongly suppressed in the B_{1g} channel. The characteristic frequency of both peaks is controlled by the superconducting order parameter Δ_S. The pseudogap scale Δ_{AF} does not show up in the pair-breaking spectrum. Except for extremely small (unrealistic) scattering rates, the two peaks merge into one and cannot be resolved experimentally even in the B_{2g} channel. An SDW-induced transition is present both below and above T_c and produces a peak at $2\Delta_{\mathrm{AF}}$. This transition is not active in B_{2g} channel.

In hole-doped compounds the two pair-breaking peaks are clearly separated. The high-energy peak frequency is controlled by the maximum gap measured in ARPES in the antinodal region.[5] It depends on both Δ_S and the pseudogap scale Δ_R. The low-energy peak appears at a frequency slightly lower than expected for a BCS superconductor with order parameter Δ_S. It is strongest in B_{2g} but it is barely visible in B_{1g}. A PG-induced *crossing* transition is present for zero or finite Δ_S and produces a peak in the spectrum at a frequency which can be very close to the high-frequency pair-breaking peak, making it difficult to disentangle both contributions in the total spectrum. This transition has higher intensity in B_{1g}. When the superconducting gap decreases (if the pseudogap scale does not change), the high-energy peak in B_{1g} barely changes its position. Similar behavior has been found in recent experiments by Guyard *et al.*[8] for a given sample with increasing temperature and for samples with the same doping but different critical temperatures due to impurity substitution.[9]

A convenient way to analyze the effect of superconductivity in the spectrum is to look at the difference response $\Delta\chi''_{B_{1g},B_{2g}}=\chi''_{B_{1g},B_{2g}}(\Delta_S)-\chi_{B_{1g},B_{2g}}$ $(\Delta_S=0)$. For realistic scattering rate values, in electron-doped cuprates the effect of PG in $\Delta\chi''_{B_{1g},B_{2g}}$ almost vanishes in the difference response except for a dip at $2\Delta_{\mathrm{AF}}$ in B_{1g} and a slight change of shape of the pair-breaking peaks. With decreasing Δ_S the peaks in $\Delta\chi''_{B_{1g}}$ and $\Delta\chi''_{B_{2g}}$ shift to lower frequencies and decrease their intensities. However, two clearly differentiated peaks appear

in the difference response in hole-doped compounds. $\Delta\chi''_{B_{2g}}$ is dominated by the low-frequency one and behaves qualitatively in the standard way (shift to lower frequencies and decrease in intensity with decreasing Δ_S). On the contrary the $\Delta\chi''_{B_{1g}}$ is controlled by the high-frequency peak. Its intensity decreases with decreasing Δ_S but its position barely depends on it (this could change to some extent if the pseudogap energy scale is very small). The appearance or not of the PG-induced (SDW or *crossing*) transition in B_{2g} channel in electron- and hole-doped cuprates originates in the different model used in both cases which folds the Brillouin zone at the AFZB in electron-doped case but does not break any symmetry in the hole-doped case.

We are not aware of any signature of the SDW transition in the Raman spectrum of electron-doped cuprates. If the SDW model discussed here is applicable, such a transition would be active in the optical conductivity, as well. In fact a peak at ~ 200 meV in the optical conductivity in the normal state has been previously associated to an SDW.[22] In hole-doped cuprates a broad feature in B_{1g} above T_c, at the same frequency at which the pair-breaking peak shows up in the superconducting state, has been observed and is considered to be the Raman signature of the pseudogap.[8]

On the contrary the different behavior of the energy scales is not a consequence of the different model used but on the different truncation of the Fermi surface produced by the pseudogap. Two energy scales, such as the ones discussed here and in Ref. 5 for hole-doped compounds, would appear in other competing models if the parameters chosen result in a single nodal Fermi pocket of size and shape similar to the ones in Ref. 5. In hole-doped cuprates the effect of the pseudogap in the spectrum is strongest in the region of **k** space which controls the high-frequency peak, destroying the Fermi surface at the Brillouin-zone edge. As a consequence, the energy of the associated pair-breaking transition increases but its intensity decreases because part of the spectral weight goes to the *crossing* transition. As this region close to $(\pi,0)$ is mainly sampled by B_{1g} channel, the spectrum in this channel is highly anomalous. On the contrary B_{2g} mostly samples the Fermi pocket; in the inner edge (the arc), the spectrum is more conventional. In electron-doped systems the pseudogap gaps the Fermi surface at the hot spots, far from $(\pi,0)$. The low- and high-frequency pair-breaking peaks originate, respectively, in the hole and electron pockets at nodal and antinodal regions. As there is a well defined Fermi surface in each pocket and a gap equal to $\Delta_{S,\mathbf{k}}$ opens in each of these Fermi surfaces, both pair-breaking peaks show up at a frequency controlled by Δ_S.

We have also calculated the spectrum for electron-doped compounds using a nonmonotonic *d*-wave superconducting order parameter in the presence of a SDW. With increasing nonmonotonicity of the superconducting order parameter, the two pair-breaking peaks first merge together and then exchange positions. Thus, for large nonmonotonicity the spectrum peaks at frequency larger in B_{2g} than in B_{1g}. For realistic values of the scattering rate, the spectrum at low energy is very similar to the one without spin-density wave.

In conclusion, although competing scenarios might be valid for hole- and electron-doped cuprates, its Raman spectrum can be very different and a careful analysis is needed. While in electron-doped cuprates the superconductivity and pseudogap are practically disentangled, this is not the case for the hole-doped cuprates. We have shown that the different truncation of the Fermi surface for hole- and electron-doped cuprates is key to understand this completely different behavior. The calculation of the Raman spectrum has been performed in the bubble approximation. We expect that vertex corrections would not modify the qualitative behavior discussed here.

Finally we note that recent experiments[12,41] suggest that in electron-doped cuprates the antiferromagnetic order in the superconducting state is short range. The SDW model used here to characterize electron-doped cuprates assumes long-range antiferromagnetism. We believe that the results reported here are still valid for short-range interactions. Some features could be broadened in a way that is similar to the nonresolution limited elastic magnetic Bragg peaks.[20] We also note that for both electron- and hole-doped systems we have kept the scattering rate constant when changing Δ_S. Experimentally the scattering rate has a nontrivial dependence in ω, **k**, and T, which could influence the spectrum to some extent.

ACKNOWLEDGMENTS

We thank T. M. Rice, A. F. Santander-Syro, T. P. Devereaux, and A. Sacuto for useful conversations. E.B. thanks the hospitality of the ETH-Zurich and ESPCI-Paris where part of this work was done. Funding from MCyT through Grant No. FIS2005-05478-C02-01, Ramon y Cajal contract, Consejeria de Educacion de la CAM, CSIC through Grant No. CG07-CSIC/ESP-2323, and I3P contract is acknowledged.

*belenv@icmm.csic.es; leni@icmm.csic.es

[1] M. R. Norman, H. Ding, M. Randeria, J. C. Campuzano, T. Yokoya, T. Takeuchi, T. Takahashi, T. Mochiku, K. Kadowaki, P. Guptasarma, and D. G. Hinks, Nature (London) **392**, 157 (1998); K. M. Shen, F. Ronning, D. H. Lu, F. Baumberger, N. J. C. Ingle, W. S. Lee, W. Meevasana, Y. Kohsaka, M. Azuma, M. Takano, H. Takagi, and Z.-X. Shen, Science **307**, 901 (2005).

[2] J. Mesot, M. R. Norman, H. Ding, M. Randeria, J. C. Campuzano, A. Paramekanti, H. M. Fretwell, A. Kaminski, T. Takeuchi, T. Yokoya, T. Sato, T. Takahashi, T. Mochiku, and K. Kadowaki, Phys. Rev. Lett. **83**, 840 (1999); S. V. Borisenko, A. A. Kordyuk, T. K. Kim, S. Legner, K. A. Nenkov, M. Knupfer, M. S. Golden, J. Fink, H. Berger, and R. Follath, Phys. Rev. B **66**, 140509(R) (2002); K. Tanaka, W. S. Lee, D. H. Lu, A. Fujimori, T. Fujii, Risdiana, I. Terasaki, D. J. Scalapino, T. P. Devereaux, Z. Hussain, and Z.-X. Shen, Science **314**, 1910 (2006); T.

Kondo, T. Takeuchi, A. Kaminski, S. Tsuda, and S. Shin, Phys. Rev. Lett. **98**, 267004 (2007).
[3] C. Kendziora and A. Rosenberg, Phys. Rev. B **52**, R9867 (1995); R. Nemetschek, M. Opel, C. Hoffmann, P. F. Müller, R. Hackl, H. Berger, L. Forró, A. Erb, and E. Walker, Phys. Rev. Lett. **78**, 4837 (1997); L. V. Gasparov, P. Lemmens, N. N. Kolesnikov, and G. Guntherodt, Phys. Rev. B **58**, 11753 (1998); S. Sugai and T. Hosokawa, Phys. Rev. Lett. **85**, 1112 (2000); M. Opel, R. Nemetschek, C. Hoffmann, R. Philipp, P. F. Müller, R. Hackl, I. Tüttõ, A. Erb, B. Revaz, E. Walker, H. Berger, and L. Forró, Phys. Rev. B **61**, 9752 (2000); M. Le Tacon, A. Sacuto, A. Georges, G. Kotliar, Y. Gallais, D. Colson, and A. Forget, Nat. Phys. **2**, 537 (2006).
[4] T. P. Devereaux and R. Hackl, Rev. Mod. Phys. **79**, 175 (2007).
[5] B. Valenzuela and E. Bascones, Phys. Rev. Lett. **98**, 227002 (2007).
[6] R. Zeyher and A. Greco, Phys. Rev. Lett. **89**, 177004 (2002).
[7] A. V. Chubukov, T. P. Devereaux, and M. V. Klein, Phys. Rev. B **73**, 094512 (2006); A. V. Chubukov and M. R. Norman, *ibid.* **77**, 214529 (2008).
[8] W. Guyard, M. Le Tacon, M. Cazayous, A. Sacuto, A. Georges, D. Colson, and A. Forget, Phys. Rev. B **77**, 024524 (2008).
[9] Y. Gallais, A. Sacuto, P. Bourges, Y. Sidis, A. Forget, and D. Colson, Phys. Rev. Lett. **88**, 177401 (2002); M. Le Tacon, A. Sacuto, Y. Gallais, D. Colson, and A. Forget, Phys. Rev. B **76**, 144505 (2007).
[10] W. Guyard, A. Sacuto, M. Cazayous, Y. Gallais, M. Le Tacon, D. Colson, and A. Forget, arXiv:0802.3166 (unpublished).
[11] N. P. Armitage, D. H. Lu, C. Kim, A. Damascelli, K. M. Shen, F. Ronning, D. L. Feng, P. Bogdanov, Z.-X. Shen, Y. Onose, Y. Taguchi, Y. Tokura, P. K. Mang, N. Kaneko, and M. Greven, Phys. Rev. Lett. **87**, 147003 (2001).
[12] S. R. Park, Y. S. Roh, Y. K. Yoon, C. S. Leem, J. H. Kim, B. J. Kim, H. Koh, H. Eisaki, N. P. Armitage, and C. Kim, Phys. Rev. B **75**, 060501(R) (2007).
[13] H. Matsui, K. Terashima, T. Sato, T. Takahashi, S.-C. Wang, H.-B. Yang, H. Ding, T. Uefuji, and K. Yamada, Phys. Rev. Lett. **94**, 047005 (2005).
[14] The presence of antiferromagnetism can depend on the annealing procedure. The gap at the hot spots and at the band folding is not observed in some reduced samples in P. Richard, M. Neupane, Y.-M. Xu, P. Fournier, S. Li, P. Dai, Z. Wang, and H. Ding, Phys. Rev. Lett. **99**, 157002 (2007); A. F. Santander-Syro, T. Kondo, S. Pailhs, A. Kaminski, J. Chang, M. Shi, L. Patthey, A. Zimmers, B. Liang, P. Li, and R. L. Greene (unpublished), which implies that a careful characterization of the sample under study is necessary.
[15] Z. Nazario and D. I. Santiago, Phys. Rev. B **70**, 144513 (2004).
[16] C. Kusko, R. S. Markiewicz, M. Lindroos, and A. Bansil, Phys. Rev. B **66**, 140513(R) (2002); T. Das, R. S. Markiewicz, and A. Bansil, Phys. Rev. Lett. **98**, 197004 (2007); T. Das, R. S. Markiewicz, and A. Bansil, arXiv:0711.1504 (unpublished).
[17] J. R. Schrieffer, X. G. Wen, and S. C. Zhang, Phys. Rev. B **39**, 11663 (1989).
[18] A.-M. S. Tremblay, B. Kyung, and D. Sénéchal, Low Temp. Phys. **32**, 424 (2006).
[19] Y. Dagan, M. M. Qazilbash, C. P. Hill, V. N. Kulkarni, and R. L. Greene, Phys. Rev. Lett. **92**, 167001 (2004).
[20] M. Matsuda, S. Katano, T. Uefuji, M. Fujita, and K. Yamada, Phys. Rev. B **66**, 172509 (2002).
[21] W. Yu, J. S. Higgins, P. Bach, and R. L. Greene, Phys. Rev. B **76**, 020503(R) (2007).
[22] Y. Onose, Y. Taguchi, K. Ishizaka, and Y. Tokura, Phys. Rev. B **69**, 024504 (2004); A. Zimmers *et al.*, Europhys. Lett. **70**, 225 (2005).
[23] G. Blumberg, A. Koitzsch, A. Gozar, B. S. Dennis, C. A. Kendziora, P. Fournier, and R. L. Greene, Phys. Rev. Lett. **88**, 107002 (2002).
[24] M. M. Qazilbash, A. Koitzsch, B. S. Dennis, A. Gozar, H. Balci, C. A. Kendziora, R. L. Greene, and G. Blumberg, Phys. Rev. B **72**, 214510 (2005).
[25] I. Eremin, E. Tsoncheva, and A. V. Chubukov, Phys. Rev. B **77**, 024508 (2008).
[26] F. Guinea, R. S. Markiewicz, and M. A. H. Vozmediano, Phys. Rev. B **69**, 054509 (2004).
[27] P. Krotkov and A. V. Chubukov, Phys. Rev. Lett. **96**, 107002 (2006).
[28] H. Matsui, K. Terashima, T. Sato, T. Takahashi, M. Fujita, and K. Yamada, Phys. Rev. Lett. **95**, 017003 (2005).
[29] T. Das, R. S. Markiewicz, and A. Bansil, Phys. Rev. B **74**, 020506(R) (2006).
[30] Q. Yuan, F. Yuan, and C. S. Ting, Phys. Rev. B **73**, 054501 (2006).
[31] C. S. Liu, H. G. Luo, W. C. Wu, and T. Xiang, Phys. Rev. B **73**, 174517 (2006).
[32] H.-Y. Lu and Q.-H. Wang, Phys. Rev. B **75**, 094502 (2007).
[33] S. Kleefisch, B. Welter, A. Marx, L. Alff, R. Gross, and M. Naito, Phys. Rev. B **63**, 100507(R), (2001).
[34] That the nonmonotonicity of the superconducting gap cannot be explained as a consequence of the opening of an antiferromagnetic gap does not mean that this nonmonotonicity does not originate in antiferromagnetic fluctuations if they are the origin of superconductivity, as discussed in Ref. 27.
[35] K.-Y. Yang, T. M. Rice, and F.-C. Zhang, Phys. Rev. B **73**, 174501 (2006).
[36] T. P. Devereaux and A. P. Kampf, Phys. Rev. B **59**, 6411 (1999).
[37] In principle, since the dispersion relation has terms of the form $\cos 2k_x + \cos 2k_y$, the B_{1g} Raman vertex could also have a contribution of the higher harmonic $\cos 2k_x - \cos 2k_y$. We have checked that this contribution does not change qualitatively the results affecting only the intensity of the Raman response.
[38] T. P. Devereaux, Phys. Rev. Lett. **74**, 4313 (1995); Phys. Rev. B **45**, 12965 (1992).
[39] F. C. Zhang, C. Gros, T. M. Rice, and H. Shiba, Supercond. Sci. Technol. **1**, 36 (1988).
[40] E. Bascones and B. Valenzuela, Phys. Rev. B **77**, 024527 (2008).
[41] E. M. Motoyama, G. Yu, I. M. Vishik, O. P. Vajk, P. K. Mang, and M. Greven, Nature (London) **445**, 186 (2007).